Geomorphic and Hydrodynamic Impacts on Sediment Transport on the Inner Louisiana Shelf

Kehui Xu[1,2,*], Jiaze Wang[3], Chunyan Li[1,2], Samuel J. Bentley[2,4], Michael D. Miner[5]

[1]Department of Oceanography and Coastal Sciences, Louisiana State University, Baton Rouge, LA, USA

[2]Coastal Studies Institute, Louisiana State University, Baton Rouge, LA, USA

[3]University of Maryland Center for Environmental Science, Cambridge, MD, USA

[4]Department of Geology and Geophysics, Louisiana State University, Baton Rouge, LA, USA

[5]The Water Institute of the Gulf, New Orleans, LA, USA

*Corresponding author: K. Xu, 2165 Energy, Coast and Environment Building, Department of Oceanography and Coastal Sciences, Louisiana State University, Baton Rouge, Louisiana 70803, USA. Email: kxu@lsu.edu; Phone: 1-225-578-0389.

Abstract

To investigate the interactions among geomorphology, hydrodynamics, and sediment dynamics on the inner shelf offshore Louisiana, multiple acoustic and optical sensors were deployed during a 58-day intermediate-energy period from May 23 to July 22, 2016. Time series results show that an elongated bathymetric "trough" between Ship Shoal and Isles Dernieres partially confines flow in the E-W (shore-parallel) direction. Warm water with lower salinity was observed in the mid to upper water column with cool water with higher salinity in the lower water column. High sediment concentrations of 1-10 g/L were observed in the bottom boundary layer during intermediate-energy conditions in response to sustained winds of up to 11 m/s, significant waves heights of up to 1.5 m, occasional 8 s period swells, and a spring tidal range of 0.6 m. The dominant current and sediment transport directions were westward during the study period. About 77% of the sediment flux occurred during three 2-day-long periods (only 10% of the observation period), revealing the nonlinear and episodic nature of sediment transport in this study area. Although intermediate-energy conditions are less energetic than hurricanes and storms, they occur more often and contribute greatly to the long-term net sediment transport. Based on preliminary estimates, ~51.0 million tons of sediment passes along the Louisiana inner shelf annually, comparable with the annual sediment exiting the Mississippi Delta and sourced from marsh edge erosion in coastal Louisiana combined. The inner shelf sediment flux is an integral part of the coastal sediment budget and may provide important mineral sediment for wetland accretion if transported onshore during storms.

Keywords: Morphodynamics; Sediment Transport; Hydrodynamics; Louisiana Shelf; Northern Gulf of Mexico; Fluid Mud

1. Introduction

1.1 Sediment transport in eroding deltaic coasts

Almost all the large river deltas (e.g., Ganges, Nile, Yellow and Yangtze) around the world are eroding because of global sea level rise, subsidence, changing hydrodynamics, declining sediment supply, levee construction and other human activities, leading to significant threats to natural, economic, and social systems in many countries (Syvitski et al., 2009; Vörösmarty et al., 2009; Bentley et al., 2016; Zhang et al. 2018a, 2018b; Xu et al., 2019; Zhang et al., 2020). Key coastal processes associated with rapid shoreline retreat, wetland loss, and expansion of bays and estuaries are the erosion of coastal shoreline and the sediment resuspension, transport, and deposition downstream in the sediment dispersal system. The transport of eroded sediment and sediment exchange between estuaries and nearby continental shelves often play a key role in the evolution of coastal morphodynamics and long-term wetland sustainability (Twilley et al., 2016; Liu et al., 2018). Many coastal protection and restoration methods have been proposed to mitigate the land loss in response to subsidence and rising sea. For instance, levee construction, sediment diversion, marsh creation and barrier island restoration have been widely used around the world and many involve the steering, delivery, and movement of sediment, either naturally to mimic sediment transport processes or manually through the pumping, dredging and replacement of sediment.

Large rivers' deltaic plains are often muddy due to their long-distance preferential transport of fine-grained sediment from large drainage basins to deltas. High sediment concentration and strong hydrodynamic conditions favor the formation of the delta plains. Defined as sediment concentration equal to or greater than 10 g/L, fluid muds can be found on many of delta plains and play a key role in sediment transport globally, such as the Yellow

(Wright et al., 1986), the Amazon (Kineke et al., 1996), the Eel (Taykovoski et al., 2007), and the Atchafalaya (Traykovski et al., 2015; Zang et al., 2020). They are often formed as “fluffy” high concentration layers at the bottom water column and separated with upper water column by lutocline. Fluid muds as well as high sediment concentration flows (here defined as 1-10 g/L) occur over a relatively short duration but can greatly impact the sediment transport process, morphology, and geological record. Studies of these high concentration sediment flows in coastal areas include those in Yellow River Delta where resuspension is due to currents (Wright et al., 1990), near Eel River shelf affected by waves (Ogston et al., 2000; Traykovski et al., 2000), and near Waiapu River affected by a combination of currents and waves (Ma et al., 2008).

Our study area is on the central Louisiana shelf where fluid mud process and subsequent fate have been reported (Oetking, 1973; Wiseman et al., 1975). Kobashi et al. (2007) reported the existence of a fluid mud layer during a tripod deployment, which was associated with the interaction of waves and fluvial sediments; they observed a fluid mud layer of 10-15 cm conspicuously influenced during a storm in late April, in which a maximum wind speed of 17 m/s and significant wave height of 2.3 m were recorded. Stone et al. (1996) showed that sediment transport processes on Ship Shoal on Louisiana shelf include contrasting non-cohesive sand and cohesive mud transport. Moreover, Stone et al. (2009) reported that the combination of spring flood discharge from the Atchafalaya River (Fig. 1) and the post-frontal meteorological conditions can lead to sediment transport to Ship Shoal. They also hypothesized that occasional sediment plume shifts from the Atchafalaya Bay to the southeast may result in the accumulation of a transient, thin, and patchy fluid mud layer on Ship Shoal with a maximum thickness of about 2-4 cm. However, tens of vibracores collected in Ship Shoal area all show clean and high-quality beach-compatible sand with essentially no mud preserved at all. These findings indicate that fluid mud may temporarily blanket Ship Shoal but is later transported elsewhere. Liu et al. (2020a) used a 3-D sediment transport model to confirm the bypass of a small amount of Atchafalaya-derived sediment over Ship Shoal on an annual time scale.

Many borrow areas have been permitted and used for sand excavations on the central Louisiana shelf in the past decade. Sand is often excavated from a target borrow area and thus a pit is formed after the dredging. In 2013, sandy muds interpreted as paleo-distributary deposits were excavated offshore Raccoon Island for the Raccoon Island Backbarrier Marsh Restoration Project (Fig. 1). Liu et al. (2020b) collected bathymetric, side-scan, and sub-bottom data in 2015 and 2018, reported a high infilling rate of 1.1 m/year in the dredge pit from 2013 to 2018 and concluded that high concentration, event-driven sediment transport is likely the key contributor for sediment infilling in this pit. On Ship Shoal, the Caminada and Block 88 dredge pits (Fig. 1) were dredged in 2016 and 2018, respectively, for barrier island restoration, and several additional dredge borrow areas on Ship Shoal are presently being excavated. Liu et al. (2019 and 2021) collected geophysical data at Caminada pit and found expanding mud patches in the deepest portions of the pit. The collective results from Kobashi et al. (2007), Stone et al. (2009), Liu et al. (2019, 2020b and 2021) and Xue et al. (2021) highlight the need to constrain the role of transient and episodic bottom boundary layer sediment transport process in infilling dredge pits on the inner shelf offshore central Louisiana. Moreover, there are multiple inner shelf shoals in the northern Gulf of Mexico such as Trinity Shoal, Tiger Shoal and Sabine Bank, which will likely be continually used for sediment borrow areas to mitigate barrier island disintegration in a regime of rapid relative sea-level rise. When implementing coastal restoration and sediment management programs, the roles of these shoals, high sediment concentration flows and fluid muds should be considered.

1.2 Regional setting

Coastal Louisiana is home to ~2 million people, supports the nation's largest commercial fishery, and supplies 90% of the nation's outer continental shelf oil and gas development and production. However, the region currently experiences about 90% of the nation's coastal wetland loss (Couvillion et al., 2011). Over the past two decades, there have been many hydrodynamics and sediment dynamics studies on the Louisiana shelf, especially on the western portion of the shelf. For example, wave supported fluid mud has been widely reported over the Atchafalaya subaqueous delta and offshore of the Chenier Plain during the passage of energetic cold fronts and tropical storms (Allison et al., 2000; Kineke et al., 2006; Jaramillo, 2008; Safak et al., 2010; Traykovski et al., 2015; Denommee et al., 2016, 2018; Zang et al., 2020). These fluid muds occurred in locations having energetic waves and abundant fine sediment, namely the shallow (<10 m) inner shelf offshore of and to the west of the Atchafalaya Bay mouth.

Xu et al. (2016a) applied a 3-D sediment transport model in Louisiana shelf and found 40 m/s model estimated winds, 18 m high waves and 45 Pa of wave-current combined shear stress during the passage of Hurricane Katrina. Using an instrumented tripod, Wright et al. (1997) concluded that fair-weather conditions in summer cannot suspend appreciable sediment in the inner Louisiana continental shelf. Li et al. (2020) reported frequent sediment resuspension during the passages of cold fronts in winter and spring and high sediment concentrations of a few g/L in Barataria Bay.

The inner Louisiana shelf is in a complex morphological zone in which river channels, bays, barrier islands and submarine shoals interact (Fig. 1). The Isles Dernieres barrier island chain experienced some of the highest shoreline retreat rates (7.0-11.2 m/year) of coastal erosion in the world from the 1890s to 2006 (McBride et al., 1992; Martinez et al., 2009; Byrnes et al., 2018; Fig. 1) prior to an aggressive barrier island restoration program implemented over the past two decades. The rapid degradation of these islands has resulted in a decrease in the ability of the island chain to protect interior wetlands from the impacts of storm surge, saltwater intrusion, an increased tidal prism, and frequent storm waves. South of Isles Dernieres, Ship Shoal is one of the largest offshore sand resources along the northern Gulf of Mexico, containing >1 billion m^3 of fine sand (Penland et al., 1990; Stone et al., 2009; Fig. 1). This shoal is approximately 50 km long and 5-12 km wide. Water depth ranges from 7-9 m on the eastern side of the shoal to approximately 3 m on the western crest.

1.3 Motivations, objectives, and scientific questions

Sediment transport fluxes on the inner Louisiana shelf are large during high-energy hurricanes but minimal during low-energy fair-weather conditions. This study targets an intermediate-energy condition in summer, with wind speeds of 1-11 m/s and wave heights up to 1.5 m. These intermediate conditions are less energetic than hurricane conditions but happen more often. Understanding the sediment transport under long-term and moderate-energy hydrodynamic conditions is important to sustain the delta and wetland.

The overarching objective of this study is to investigate how geomorphology and hydrodynamics (waves, tides, and currents) impact the sediment transport processes in the inner Louisiana shelf. The primary research scientific questions are: (1) How do Isles Dernieres and Ship Shoal impact current direction and magnitude during summer? (2) How does Ship Shoal impact the wave characteristics on the inner shelf? (3) How do waves and currents contribute to the combined shear stress for sediment resuspension? (4) Can the sediment concentration near bottom boundary layer reach the level of 1-10 g/L during moderate energy summer? and (5) What are the sediment transport directions and fluxes?

2. Methods

2.1 Tripod observation using optical and acoustic sensors

Multiple optical and acoustic sensors mounted to a tripod were deployed at Station R1 in a water depth of ~ 8 m on May 23, 2016 and retrieved on July 22, 2016 (Fig. 1). A downward-looking Acoustic Doppler Velocimeter (ADV), an upward-looking Acoustic Doppler Current Profiler (ADCP), a wave gauge, and two optical backscatter sensors (OBS3 and OBS5) were used over this 58-day observational period. The downward looking Sontek 5-MHz ADV Ocean was deployed to capture time-series seabed elevation change as well as pressure, wave, and current conditions at 0.63 m above bed (mab). The distance from ADV Ocean probes to water-sediment interface was measured acoustically; when assuming the elevation of probe attached to a rigid tripod platform is fixed, the time-series seabed elevation change was calculated. An upward-looking 1200 kHz RDI Sentinel ADCP was used to measure current velocities in the water column. An OBS-3A was used to measure turbidity, temperature, pressure, and conductivity at 0.52 mab; sea water temperature and salinity data from OBS-3A were used but turbidity data were not used in this study due to heavy biofouling on this turbidity sensor. An OBS5+ sensor was mounted at about 0.10 mab to capture high turbidity close to seabed and experienced relatively less impact from biofouling. See Table 1 for the detailed parameters and settings of these sensors. These sensors have been used in multiple estuaries and shelf areas in Louisiana and some data analysis methods can be found from Wang et al. (2018, 2019), Li et al. (2020) and Xu et al. (2020).

An upward-looking 600 kHz RDI Sentinel ADCP was also used to measure current velocities in the water column at Station CSI06 to measure sea water temperature and waves. CSI06 has been one of the ocean-observing stations of the Wave-Current-Surge Information System for Coastal Louisiana (WAVCIS) of Louisiana State University (LSU). Wind speed and directions were collected at an elevation of ~10 m. More details of WAVCIS system can be found at www.wavcis.lsu.edu.

2.2 Laboratory methods

"Local" surficial sediment samples were collected at Station R1 using a clam shell grabber. Five replicates from R1 were analyzed using a Beckman Coulter LS 13 320 laser particle size analyzer, following the methods of Xu et al. (2014 and 2016b). A portion of the sediment was mixed with water in a chamber for the calibration of OBS5 data to convert from Nephelometric Turbidity Unit (NTU) to concentration of g/L and the details are in Wang et al. (2018) and Li et al. (2020).

2.3 Data Analysis

The Atchafalaya River's water discharge data at Simmesport of Louisiana were downloaded from USGS website at https://waterdata.usgs.gov/nwis/uv?site_no=07381490. Wave data collected using two upward-looking ADCPs at R1 and CSI06 were analyzed using WavesMon software from Teledyne RD Instruments. Wave direction was defined as where the wave comes from (e.g., 0 degree is from N). All other tripod sensor data were analyzed using MATLAB. All the data collected from May 23, 2016 to July 22, 2016 were analyzed, and three

2-day long periods were used for comparison. These three periods were: May 27-29 (defined as P1), June 7-9 (P2) and July 4-6 (P3) of the year 2016.

2.4 1-D vertical modeling method

Since most sensor measurements in this study were at fixed points (except ADCP) on the tripod, a mathematical model is needed to estimate the vertical profiles of velocity and sediment concentration and to calculate depth-integrated sediment fluxes. The Styles & Glenn 1-D bottom boundary layer model (Styles and Glenn, 2000) was used in this study to compute the roughness, eddy viscosity, velocity, and non-cohesive sediment concentration profiles at Station R1. This model included 3-layer eddy viscosity profiles that made the model continuous in the eddy viscosity at the top of the wave boundary layer. The inputs of this model included time, wave orbital velocity, wave excursion amplitude, mean current velocity, height above seabed, and sediment grain size. Both current-only and wave-current-combined shear stresses were calculated in the model. Recent two applications of this Styles & Glenn model are in the muddy Fourleague Bay of Louisiana in Wang et al. (2019) and the sand-mud mixed Barataria Bay of Louisiana in Li et al. (2020).

Over the years, many bottom boundary layer models have been developed for muddy and sandy environments. Based on Madsen (1994) and others, for instance, the Styles & Glenn (2000) model was developed to include multiple improvements in the stratified wave and current boundary layer and has been adopted in a 3-D sediment transport model in Regional Ocean Modeling System (Warner et al., 2008). Several moveable bed routines developed by Wiberg and Harris (1994) and Harris and Wiberg (2001) were also added to this 3-D model. However, modeling 3-D sediment transport is beyond the scope of this study. Since there is a lack of field measurements of floc size, organic matter, bed erodibility and consolidation, cohesive sediment behavior like flocculation (aggregation, breakup, and disaggregation), bed consolidation and swelling are not in the 1-D modeling work of this study either.

3. Results

3.1 River discharge, salinity, temperature, and water level

The 58-day tripod observational period happened during the waning stage of Atchafalaya River discharge, decreasing from about 9500 to around 5000 m^3/s (Fig. 2A). From May 23 to July 22, 2016, water temperature in bottom water column at Station R1 had been increasing, possibly due to the increased solar radiation from early to middle summer in 2016 (Fig. 2B). Salinity of bottom water varied between 22 and 30. Tidal levels at R1 displays a typical diurnal tidal signal; the tidal range in spring tide reached 0.6 m whereas that of neap tides was only 0.2 m (Fig. 2C).

3.2 Winds and currents

Wind speed at CSI06 varied between 1 and 11 m/s from May 23 to July 22, 2016 (Fig. 3A). Wind directions were stable during more than half of this period but were highly rotational during P1 and P2 (Fig. 3B); the directions during the period from June 22 to July 3, 2016 rotated daily, possibly in response to the sea and land breezes. The E-W and N-S bidirectional currents measured by ADCP at 8-m deep Station R1 shows a strong impact from tides, with E-W being much faster than N-S ones in the upper half of water column (dark red and dark blue in Fig. 3C&D). Over the same period, ADCP data were collected at 20-m deep Station CSI06; the E-W and N-S currents at Station CSI06 were comparable and fast currents occurred near sea surface, especially during the spring tides during which tidal ranges were large (Fig. 4).

3.3 Waves

Wind speed and wave data from stations R1 and CSI06 show that high winds appeared to have corresponded with fast moving currents and peak wave heights (Fig. 5A, B&C). Wave periods from both stations shared the same increasing and decreasing trend (Fig. 5D). Most waves at the two stations were propagated from the south, southwest and southeast toward the land (Fig. 5E). During P2, wave periods increased rapidly from 4 to 8 s during which wind speeds were less than 5 m/s, indicating some swells propagating from deep ocean to the inner Louisiana shelf but unrelated to local winds.

3.4 Sediment grain size

Laser grain size data of surficial sediment sample shows a muddy texture at Station R1. The percentages of sand, silt and clay were around 9.9%, 60.7% and 29.4%, respectively (Fig. 6). This finding was consistent with the results of a large surficial grain size database created by the usSEABED project (Williams et al., 2006; Fig. 7). Both Isle Dernieres and Ship Shoal were sand-dominated, but sediment between them were generally clayey silt with some sandy patches (Fig. 7). Station CSI06 was in a relatively fine-grained area with variable sand percentages of 0-40%.

3.5 Sediment transport

The 1-D vertical Styles & Glenn model was used to compute shear stress (wave only, current only and wave-current combined) and sediment concentration profile in many vertical layers at Station R1. The wave-current combined shear stress during P1 and P2 exceeded 1 Pa, triggering strong sediment resuspension events (Fig. 8A&B). Both currents and waves contributed to the combined wave-current shear stresses (Fig. 8A). Both modeled and OBS5-calibrated sediment concentrations exceeded 1 g/L during P1 and P2. Interestingly, OBS5-calibrated concentration reached ~10 g/L during multiple episodes from June 2-10, 2016. Although both observed OBS5 and modeled sediment concentrations reached sediment concentrations levels at 1-10 g/L, there were a few mismatches during events and further explanations are in Section 4.5.

4. Discussion

4.1 Morphologic impact on currents and waves

Between Ship Shoal and Isles Dernieres, Station R1 is in an elongated "trough" (or a strait) which is about 50 km long and 15 km wide (Fig. 1). Such a morphologic setting plays a key role in controlling the circulation and trajectory of coastal currents. Fig. 9 shows a comparison of current directions between R1 and CSI06. The prevailing current directions at R1 were along E-W, with a dominating westward current. This is consistent with a modeling result of yearly westward longshore current from in Xu et al. (2011). However, the current directions at CSI06, located outside of the trough, were highly variable with a dominant direction toward NE.

Wave heights, periods, and directions in R1 and CSI06 shared some similar response to high wind speed events (Fig. 5). When comparing wave heights at R1 with these at CSI06, however, during most of the observational period, the heights of CSI06 were greater than those of R1 (Fig. 10A). The differences in heights between two stations were small (near the black 1:1 line) when wave heights at R1 were less than 0.4 m, but the differences were large when heights at R1 were greater than 0.8 m (Fig. 10A). These height differences revealed not only the decreasing water depths from 20 m at CSI06 to 8 m at R1 but also some possible wave breaking on top of Ship Shoal when waves propagated onshore. Wave periods at R1 were very close but generally shorter than these at CSI06 (Fig. 10B). Wave directions at R1 clustered at 100-200 degrees, but the directions at CSI06 were 100-270 degrees (Fig. 10C). The paucity of waves coming from 200-270 degrees (from SW) at R1 presumably indicates the wave sheltering by western crest of Ship Shoal (brown in Fig. 1).

4.2 Temperature, salinity, wind, and wave

Time-series temperature and salinity data can be used to analyze the mixing of multiple water masses in coastal ocean. Fig. 11 displays the relationship between temperature and salinity over three periods: May 25-28, May 28-June 7 and June 7-21 of 2016. The rightward shifting of scattered symbols on Fig. 11 from May 25-28 to June 7-21 clearly demonstrates a 3-degree warming from early to middle summer of 2016. Interestingly, during three periods, temperature and salinity oscillated between "warm and less saline" water and "cold and salty" water. Unfortunately, no temperature and salinity data were collected in the middle or upper water columns. It is likely that cold and salty water is from one bottom water mass and warm and less saline water is from another distinct water mass in the middle or upper water column.

During P1, wind directions were from SE and the average wind speeds were 6.9 m/s (Table 2). The maximum westward currents reached 0.43 m/s and wave heights were 0.85 m. Both alongshore and cross-shore velocity profiles were rapid at the sea surface and slower near bottom and sediment concentrations near bottom boundary layer reached 1-4 g/L (Fig. 12). During P2, wind directions were highly rotating, maximum westward currents were only 0.25 m/s, and average wave periods were 6.5 s due to the impact of swells. Sediment concentration profiles of P1 and P2 were comparable. During P3, winds were from SW at 6.6 m/s, alongshore currents were eastward, and sediment concentrations near bottom were generally less than 1.5 g/L.

4.3 Morphologic impact on sediment fluxes

The 50-km long trough between Ship Shoal and Isle Dernieres not only influences hydrodynamics but also sediment transport. Depth-integrated sediment fluxes were calculated at R1 along both alongshore and cross-shore directions. For alongshore fluxes, westward sediment transport exceeded 5 kg/m/s during P1 and P2 (Fig. 13). During P3, however, sediment transport was eastward and reached 2 kg/m/s. Despite the well-documented long-term net westward transport, short-term eastward transport can happen in response to strong winds from SW. Cross-shore fluxes were always less than the alongshore fluxes during the entire observational period (Fig. 13C). Both onshore and offshore fluxes were observed but the net transport were southward over the 58-day period. There are two possible primary sources for the sediment being transported southward: 1) barrier shoreface ravinement (Miner et al., 2009a) and 2) sediment export from the estuarine system and eroding interior wetlands via tidal inlets. About 77% of sediment fluxes occurred during all three periods (P1-P3, a total of only 6 days) over the 58-day observational period. This highlights the episodic and non-linear nature of sediment transport in the area.

4.4 Implications to sediment budget and coastal restoration

After calculating sediment concentrations and velocity along many vertical layers in Styles & Glenn model, the product of concentration (kg/m^3) and velocity (m/s) yields sediment flux which is in kg/m^2/s. When depth-integrated, sediment flux unit becomes kg/m/s. In this sediment flux calculation, velocity at 0.63 mab was directly from the measurement of ADV Ocean and used in calculating the velocity profile in Styles & Glenn model. Sediment concentration profile was calculated using this model as well.

A simple calculation discussed below provides for an estimate of the sediment budget along an "conceptual" N-S cross section passing R1 in the "trough" between Ship Shoal and Isle Dernieres (Fig. 1). Since our tripod measurements were hourly, this unit of kg/m/s needs to be converted to kg/m. Because the width of the trough is roughly 15 km, the flux should be multiplied by 15,000 m. Over the 58-day observational period, the net alongshore sediment flux was ~150 kg/m/s toward west (Fig. 13C), and the flux crossing the trough was:

$$[150 \text{ kg/m/s} \times (3600 \text{ s/1 h}) \times 15{,}000 \text{ m}] / 58 \text{ days} = 8.1 \times 10^{9} \text{ kg/ 58 days}$$

Then the unit can be converted to:

$$(8.1 \times 10^{9} \text{ kg/ 58 days}) \times (365 \text{ days/ 1 year}) \times (1 \text{ ton/1000 kg}) = 51.0 \text{ million ton/year}$$

The sources of errors for the above flux calculation can be from both velocity and sediment concentration. The accuracy of Sontek ADV Ocean measurements was 1% of measured velocity, and thus contributed to minimal error to the flux calculation. Sediment concentration, however, can vary several orders of magnitude, from 0.01 g/L to 10 g/L, in our model simulations and is highly sensitive to the inputs of grain size, critical shear stress, wave and current. In addition, the spatial variation along the "conceptual" N-S cross section is not captured in the calculation. Couvillion et al. (2011) did a trend analysis from 1985 to 2010 and reported an average wetland loss rate of 16.57 mile^2/year in coastal Louisiana, which was 42.92 km^2/year. Assuming an erosional depth of 1.0 m (many Louisiana bays are 2-4 m deep), a porosity of 0.5, and a sediment density of 2650 kg/m^3, that would yield a sediment of 56.8 million ton/year. It should be noted that some sediment eroded from the marsh edge may deposit to nearby marsh and bay bottom to fill in the new accommodation space created by fast land subsidence and sea level rise and never reach the inner shelf environment. Based on seafloor change analysis, between 1890 and 2006, Miner et al. (2009a) estimated that ~1.2×10^9 m^3 of sediment were eroded from the Isles Dernieres and updrift Caminada Headland shoreface during the 125-year period covered by historical data. Averaged over an annual timescale, this shoreface ravinement would contribute approximately 9.8×10^6 m^3 of sediment annually; however, the contribution is somewhat episodic with tropical cyclones being the major driving forces that greatly increase the magnitude of shoreface ravinement (Miner et al., 2009b; Allison et al., 2010). Allison et al. (2012) reported that during 2008-2012 sediment reaching the modern bird-foot Mississippi Delta was around 38.1 million ton/year and that reaching the Wax Lake Delta and Atchafalaya Delta totaled about 48.3 million ton/year. Our estimate, however, shows that the alongshore sediment flux in the inner shelf is comparable to both the modern river supplies and the sediment eroded from marsh edge and barrier shoreface, all in the magnitude of 10s million ton/year.

This alongshore sediment flux is tremendous and while some may be reworked by storms and transported landward, the net export signals a major deficit in the fine-grained sediment budget for coastal Louisiana every year. Over the past three decades, sediment has been dredged for coastal barrier island restoration and mud has been used for marsh creation (CPRA, 2012). As mentioned in Section 1, the Raccoon Island dredge pit was about 1 km from Station R1 and located in a paleo river channel and the Caminada and Block 88 dredge pits were on top of the Ship Shoal (see Fig. 1 for three pits). Liu et al. (2019) found muddy patches accumulation on the bottom of Caminada pit. Liu et al. (2020a) reported 100% infilling of muddy sediment at Raccoon Island dredge pit six years after dredging and a rapid sediment infilling rate of 1.1

m/year. These high sediment accumulation rates in Raccoon Island pit corroborated the abundance of muddy sediment passing our study area and thus sediment availability for pit infilling.

Fluid mud has been reported on the western Louisiana shelf in many publications (e.g., Kemp, 1986; Kemp and Wells, 1987; Roberts et al., 2002; Rotondo and Bentley, 2003; Traykovski et al., 2015; Zang et al., 2020). This study revealed a new near-fluid-mud concentration sediment flow on the inner shelf offshore central Louisiana, a process that was thought to be associated with strong, storm-associated currents on the shelf (Stone et al., 2009; Allison et al., 2010). However, the timing of the observations reported herein with measurements acquired during moderate-energy (non-storm) periods indicate that high concentration sediment flows on the inner shelf can occur on Louisiana shelf. Although being less energetic than storm/hurricane conditions, moderate conditions occur more often, take place over a longer duration, and play a key role in transporting sediment and shaping coastal morphology.

4.5 Limitations, ongoing and future Work

The turbidity data collected using OBS3 in this study were not usable due to heavy biofouling in summer, and the data collected using OBS5 was also limited. In the future, an OBS sensor equipped with a self-cleaning brush is needed for such a marine environment (e.g., Li et al., 2020). The Styles & Glenn sediment model (Styles and Glenn, 2000) is 1-D vertical, does not include any cohesive sediment function, and cannot capture any sediment advection from submarine shoals, barriers, bays, and rivers. Moreover, it is well known that optical sensors are sensitive to mud as well as floating organic matter in the water column, but not so sensitive to sand. Organic matter is less dense than minerals and can cause significant overestimation of OBS which is purely based on light measurement. When there is a resuspension event, the Styles & Glenn model computes a flux contributed significantly by sand, but such flux can be 'overlooked' by the OBS sensor. The mismatch of sediment concentration between OBS5 and modeled sediment concentration around June 5, 2016 in Fig. 8C highlights the need of improved field measurements and 3-D sediment transport model. Besides optical and acoustic (e.g., ADCP) measurements of sediment concentrations, sequential portable samplers can be used to collect in-situ time-series water samples in the field. Zang et al., (2020) recently added fluid mud process in the 3-D sediment transport model in Regional Ocean Modeling System (https://www.myroms.org/). Liu et al. (2020b) accomplished high-resolution sediment transport model runs for Ship Shoal, Terrebonne Bay and Atchafalaya Bay areas and more in-depth model analysis will be performed to calculate bay-shelf sediment exchange and alongshore and cross-shore sediment fluxes. More future studies are needed to investigate the frequencies and durations of high sediment concentration sediment flows in bays and inner shelves to support future coastal restoration effort to dredge sediment for marsh creation. Moreover, the studies of cohesive sediment behavior like flocculation and bed consolidation are very much needed, especially the measurements of floc size, density and settling velocity as well as the measurements of seabed erodibility. Moreover, this study was based on limited measurements of bottom boundary layer on only one tripod. In the future, multiple tripods are needed to better represent the spatial variations.

5. Conclusions

Multiple optical and acoustic sensors were used in this study to collect hydrodynamic and sediment data in inner Louisiana shelf. The 50-km long and 15-km wide trough between Ship

Shoal and Isle Dernieres played a key role in controlling not only currents but also sediment transport. Dominant current and sediment transport directions were both westward in the study period, leading to a major "deficit" in the fine-grained sediment budget for coastal Louisiana. Bottom water at Station R1 was generally under the combined impacts of both warm and less saline water mass in the middle/upper water column and cold and salty water mass in the bottom. Wave heights, periods, and directions at Station R1 shared similarities with CSI06; higher waves occurred in both stations in response to strong local winds and episodic long-period swells occurred in both stations. Wind directions played an important role in driving surface current and sediment transport direction. Approximately 51.0 million tons of sediment can pass inner Louisiana shelf in a year, comparable with sediment exiting the Mississippi Delta and the sediment eroded from marsh edge and barrier shoreface in coastal Louisiana. Sediment concentrations during multiple periods in the moderate-energy conditions reached a level of 1-10 g/L, a process that was previously thought to require hurricane or storm conditions.

Acknowledgements

We are grateful to the Editors of Geomorphology and four guest editors of this special issue (Drs. Qiang Yao, Kam-biu Liu, Weiguo Zhang and Yan Liu). This study is supported by the U.S. Department of the Interior, Bureau of Ocean Energy Management, Coastal Marine Institute, Washington DC (under Cooperative Agreement Numbers M14AC00023, M15AC000015 and M16AC00018) as well as by NOAA (NOS-IOOS-2016-2004378). Many thanks to the Field Support Group of Coastal Studies Institute of Louisiana State University and Dr. Jeffrey Obelcz for tripod deployment and sediment sample collection. We thank Dr. Haoran Liu for doing laser grain size analysis for this study.

Table Captions

Table 1, Measurement parameters and settings of optical and acoustic sensors used in this study. T is temperature, S is salinity, V is velocity, and P is pressure. mab = meters above bed.

Table 2. Comparison of driving mechanisms of hydrodynamics and sediment dynamics during three periods P1, P2 and P3. Tide, wind, and wave data are averaged from Figs. 3, 4 and 6 respectively. Maximum longshore current speed averages are from Fig. 8. Cumulative longshore sediment fluxes are from Figs. 12 and 13.

Figure Captions

Fig. 1. Bathymetric map of the study area on the Louisiana inner shelf, including tripod Station R1, WAVCIS Station CSI06, Ship Shoal, Isles Dernieres, nearby river and bays, as well as three dredge pits (Raccoon Island, Caminada and Block 88) for coastal barrier restoration. Caminada pit is located in South Pelto block and used for Caminada Headland restoration project. Bathymetric data are from ETOPO1 (https://www.ngdc.noaa.gov/mgg/global/).

Fig. 2. (A) Time series of river water discharge from a gauging station at Simmesport of Louisiana, (B) temperature and salinity from OBS3A on a tripod at Station R1, and (C) tidal variation in relative to the mean water level from ADCP data collected at R1over the entire deployment period. Shaded boxes P1, P2 and P3 are three comparing periods.

Fig. 3. Time series of (A) wind speeds and (B) directions from CSI06, and (C) east(+)/west(-) and (D) north(+)/south(-) velocities from an upward looking ADCP at Station R1. mab= meters above bed. Black lines are water level. Shaded boxes P1, P2 and P3 are three comparing periods.

Fig. 4. Time series of east(+)/west(-) and (D) north(+)/south(-) velocities from an upward looking ADCP at Station CSI06. mab= meters above bed. Black lines are water level.

Fig. 5. Time series of (A) wind speeds at CSI06, (B) horizontal velocities of ADCP and ADV at different elevations of Station R1, (C) significant wave heights, (D) significant wave periods and (E) directions at both R1 and CSI06. P1, P2 and P3 are three comparing periods.

Fig. 6. Grain size distribution of surficial sediment collected at tripod Station R1. Grey lines are five replicates and bold black line is the average of five replicates.

Fig. 7. Sandy percentages of surficial sediment based on usSEABED database from Williams et al. (2006). The map shows tripod Station R1, WAVCIS Station CSI06, Ship Shoal, Isles Dernieres, as well as three dredge pits (Raccoon Island, Caminada, and Block 88) for costal barrier restoration. Bathymetric data are from ETOPO1 (https://www.ngdc.noaa.gov/mgg/global/).

Fig. 8. Time series of (A) wave-current combined and current-only shear stresses calculated using Styles & Glenn (2000) model, (B) modeled sediment concentration, (C) modeled and measured (using OBS5) sediment concentration at 0.10 mab. mab= meters above bed. P1, P2 and P3 are three comparing periods.

Fig. 9. The frequencies of directions of depth-averaged currents in Station R1 and CSI06 over the 58-day observational period.

Fig. 10. Comparisons of wave heights (A), periods (B) and directions (C) between R1 and CSI06 over the 58-day observational period.

Fig. 11. The relationship between temperature and salinity at Station R1 during three periods in 2016.

Fig. 12. Alongshore and cross-shore current velocities and sediment concentration during three comparing periods of P1, P2 and P3, as well as the averages of entire 58-day observation. See Table 2 for details.

Fig. 13. (A) Alongshore and (B) cross-shore depth-integrated sediment fluxes at tripod Station R1. (C) cumulative longshore and cross-shore fluxes. P1, P2 and P3 are three comparing periods.

References

Allison MA, Kineke GC, Gordon ES, Goni MA, 2000. Development and reworking of a seasonal flood deposit on the inner continental shelf off the Atchafalaya River. Continental Shelf Research 20(16):2267–2294. https://doi.org/10.1016/S0278-4343(00)00070-4

Allison, M. A., Ramirez, M. T., & Meselhe, E. A., 2014. Diversion of Mississippi River water downstream of New Orleans, Louisiana, USA to maximize sediment capture and ameliorate coastal land loss. Water resources management, 28(12), 4113-4126.

Allison, MA, Dellapenna, TM, Gordon, ES, Mitra, S., and Petsch, ST, 2010. Impact of Hurricane Katrina (2005) on shelf organic carbon burial and deltaic evolution: Geophysical Research Letters, v. 37, L21605.

Bentley, S. J., Blum, M. D., Maloney, J., Pond, L., & Paulsell, R., 2016. The Mississippi River source-to-sink system: Perspectives on tectonic, climatic, and anthropogenic influences, Miocene to Anthropocene. Earth-Science Reviews, 153, 139-174.

Blum, M. D., & Roberts, H. H., 2009. Drowning of the Mississippi Delta due to insufficient sediment supply and global sea-level rise. Nature Geoscience, 2(7), 488.

Byrnes, M.R., Berlinghoff, J.L., Griffee, S.F, and Lee, D.M., 2018. Louisiana Barrier Island Comprehensive Monitoring Program (BICM): Phase 2 – Updated Shoreline Compilation and Change Assessment 1880s to 2015: Prepared for Louisiana Coastal Protection and Restoration Authority by Applied Coastal Research and Engineering, Metairie, LA, 46 p plus appendices. https://cims.coastal.la.gov/RecordDetail.aspx?Root=0&sid=21641#

Coleman, J.M., Prior, D.B., and Garrison, L.E., 1980. Subaqueous sediment instabilities in the offshore Mississippi River delta: United States Department of Interior, Bureau of Land Management, New Orleans Outer Continental Shelf Office, Open-File Report 80-01, 60 p.

Couvillion, B.R., J.A. Barras, G.D. Steyer, W. Sleavin, M. Fischer, H. Beck, N. Trahan, B. Griffin, & D. Heckman, 2011. Land area change in coastal Louisiana from 1932 to 2010: U.S. Geological Survey Scientific Investigations Map 3164, scale 1:265,000, 12 p. pamphlet.

Coastal Protection and Restoration Authority (CPRA), 2012. Louisiana's Comprehensive Master Plan for a Sustainable Coast. Coastal Protection and Restoration Authority of Louisiana, Baton Rouge, LA. 189 pp.

Denommee KC, Bentley SJ, Harazim D, Macquaker JHS, 2016. Hydrodynamic controls on muddy sedimentary fabric development: Atchafalaya Chenier plain Subaqueous Delta. Mar Geol 382:162–175. https://doi.org/10.1016/j.margeo.2016.09.013

Denommee, K. C., Bentley, S. J., & Harazim, D., 2018. Mechanisms of muddy clinothem progradation on the Southwest Louisiana Chenier Plain inner shelf. Geo-Marine Letters, 38(3), 273-285. https://doi.org/10.1007/s00367-017-0525-3.

Harris, C.K., Wiberg, P.L., 2001. A two-dimensional, time-dependent model of suspended sediment transport and bed reworking for continental shelves, Computers & Geosciences, 27, 675-690.

Jaramillo S, Sheremet A, Allison MA, Reed A.H., & Holland K.T., 2009. Wave-mud interactions over the muddy Atchafalaya subaqueous clinoform, Louisiana, United States: wave-supported sediment transport. Journal of Geophysical Research: Oceans 114(C4):C04002. https://doi.org/10.1029/2008JC004821

Kemp, G. P., 1986. Mud deposition at the shoreface: wave and sediment dynamics on the Chenier Plain of Louisiana: Ph.D. dissertation, Louisiana State University, 146 p.

Kemp, G.P., and Wells, J.T., 1987. Observations of shallow-water waves over a fluid mud bottom: implications to sediment transport: Coastal Sediments ’87, p. 363-378.

Khalil, S. M., Freeman, A. M., & Raynie, R. C., 2018. Sediment management for sustainable ecosystem restoration of coastal Louisiana. Shore & Beach, 86(1), 17.

Kineke, G. C., R. W. Sternberg, and J. H. Trowbridge, 1996. Fluid - mud processes on the Amazon continental shelf, Continental Shelf Research, 516, 667 – 696, doi:10.1016/0278-4343(95)00050-X.

Kobashi, D., 2009. Bottom boundary layer physics and sediment transport along a transgressive sand body, ship shoal, south-central Louisiana: implications for fluvial sediments and winter storms, Ph.D. Dissertation, Louisiana State University, Baton Rouge, LA. 155 pp.

Li, G, Xu, K, Xue, ZG, Liu, H, Bentley, SJ, 2020. Hydrodynamics and sediment dynamics in Barataria Bay, Louisiana, USA, Estuarine, Coastal and Shelf Science, 107090. https://doi.org/10.1016/j.ecss.2020.107090

Liu, H., Xu, K.H., Li, B., Han, Y., Li, G., 2019. Sediment Identification Using Machine Learning Classifiers in a Mixed-Texture Dredge Pit of Louisiana Shelf for Coastal Restoration. Water, 11, 1257. https://www.mdpi.com/2073-4441/11/6/1257.

Liu, H., Xu, K.H., Ou, Y., Bales, R., Zang, Z., Xue, Z.G., 2020a. Sediment Transport near Ship Shoal for Coastal Restoration in the Louisiana Shelf: A Model Estimate of the Year 2017–2018. Water 2020, 12, 2212.

Liu, H., Xu, K.H., Wilson, C., 2020b. Sediment infilling and geomorphological change of a mud-capped Raccoon Island dredge pit near Ship Shoal of Louisiana shelf, Estuarine, Coastal and Shelf Science, 245, 106979. https://doi.org/10.1016/j.ecss.2020.106979.

Liu, H., Xu, K., Wilson, C., Bentley, S., Xue, Z., Zhang, Z., 2021. Geomorphologic response and patchy mud infilling in a sandy dredge pit in Ship Shoal, Louisiana shelf, USA. Geomorphology, 107983. https://doi.org/10.1016/j.geomorph.2021.107983

Liu, K., Chen, Q., Hu, K., Xu, K., & Twilley, R. R., 2018. Modeling hurricane-induced wetland-bay and bay-shelf sediment fluxes. Coastal Engineering, 135, 77-90.

Ma, Y., L.D. Wright, and C.T. Friedrichs, 2008. Observations of sediment transport on the continental shelf off the mouth of the Waiapu River, New Zealand: Evidence for current-supported gravity flows. Continental Shelf Research, 28: 516-532. https://doi.org/10.1016/j.csr.2007.11.001

Madsen, O.S., 1994. Spectral wave–current bottom boundary layer flows. In: Coastal Engineering 1994. Proceedings of the 24th International Conference on Coastal Engineering Research Council, Kobe, Japan, pp. 384–398.

Maloney, J. M., Bentley, S. J., Xu, K., Obelcz, J., Georgiou, I. Y., & Miner, M. D., 2018. Mississippi River subaqueous delta is entering a stage of retrogradation. Marine Geology, 400, 12-23.

Martinez L, O'Brien S, Bethel M, Penland S, Kulp M, 2009. Louisiana barrier island comprehensive monitoring program (BICM), vol 2. Shoreline changes and barrier island land loss 1880 s to 2005. Univ New Orleans Pontchartrain Inst Environ Sci Tech Rep. Submitted to Louisiana Office of Coastal Protection and Restoration, Baton Rouge, LA. https://cims.coastal.la.gov/RecordDetail.aspx?Root=0&sid=1025

McBride RA, Penland S, Hiland MW, Williams SJ, Westphal KA, Jaffe BE, Sallenger AH Jr, 1992. Analysis of barrier shoreline change in Louisiana from 1853 to 1989. In: Williams SJ, Penland S, Sallenger AH Jr (eds) Louisiana barrier island erosion study. Atlas of shoreline changes in Louisiana from 1853 to 1989. US Geol Surv and Louisiana State Univ Misc Investig Series I-2150-A, pp 36–97

Miner, M.D., Kulp, M.A., FitzGerald, D.M., Flocks, J.G., and Weathers, H.D., 2009a, Delta lobe degradation and hurricane impacts governing large-scale coastal behavior, South-central Louisiana, USA: Geo-Marine Letters, v. 29, p. 441- 453.

Miner, MD, Kulp, MA, FitzGerald, DM, and Georgiou, IY, 2009b, Hurricane-associated ebb-tidal delta sediment dynamics: Geology, v 37, no. 9, p 851- 854.

Obelcz, J., Xu, K.H., Bentley, S.J., O'Connor, M., Miner, M., 2018. Mud-capped dredge pits: An experiment of opportunity for characterizing cohesive sediment transport and slope stability in the northern Gulf of Mexico, Estuarine, Coastal and Shelf Science, 208, 161-169.

Oetking, P., 1973. Currents on the nearshore continental shelf of south-central Louisiana: Offshore Ecology Investigation, Gulf Univ. Res. Consort., v. II, p. 41.

Ogston, A. S., D. A. Cacchione, R. W. Sternberg, and G. C. Kineke, 2000. Observations of storm and river flood - driven sediment transport on the northern California continental shelf, Cont. Shelf Res., 20, 2141 – 2162, doi:10.1016/S0278-4343(00)00065-0.

Penland, S., Suter, J.R., Ramsey, K.E., McBride, R.A., Williams, S.J., and Groat, C.G., 1990. Offshore Sand Resources for Coastal Erosion Control in Louisiana: Gulf Coast Association of Geological Societies Transactions, v. 40, p. 721-731.

Peyronnin, N. S., Caffey, R. H., Cowan, J. H., Justic, D., Kolker, A. S., Laska, S. B., McCorquodale, A., Melancon, E., Nyman, J.A., Twilley, R.R., & Visser, J. M., 2017. Optimizing sediment diversion operations: working group recommendations for integrating complex ecological and social landscape interactions. Water, 9(6), 368.

Roberts, H.H., S. Bentley, J.M. Coleman, S.A. Hsu, O.K. Huh, K. Rotondo, M. Inoue, L.J. Rouse Jr., A. Sheremet, G. Stone, N. Walker, S. Welsh, and W.J. Wiseman Jr., 2002. Geological framework and sedimentology of recent mud deposition on the eastern Chenier Plain coast and adjacent inner shelf, western Louisiana: Transactions, Gulf Coast Association of Geological Societies, v. 52, p. 849-859.

Robichaux, P., Xu, K.H., Bentley, S. J., Miner, M., Xue, Z., 2020. Morphological evolution of a mud-capped dredge pit on the Louisiana shelf: Nonlinear infilling and continuing consolidation. Geomorphology, https://doi.org/10.1016/j.geomorph.2019.107030, 107030.

Rotondo, K.A. and S.J. Bentley, 2003. Deposition and resuspension of fluid mud on the western Louisiana inner shelf: Transactions, Gulf Coast Association of Geological Societies, v. 53, p. 722–731.

Sahin, C., I. Safak, A. Sheremet, and A. J. Mehta, 2012. Observations on cohesive bed reworking by waves: Atchafalaya Shelf, Louisiana, Journal of Geophysical Research, 117, C09025, doi:10.1029/2011JC007821.

Sheremet A, Jaramillo S, Su SF, Allison MA, & Holland KT, 2011. Wave-mud interaction over the muddy Atchafalaya subaqueous clinoform, Louisiana, United States: wave processes. Journal of Geophysical Research: Oceans 116(C6):C06005. https://doi.org/10.1029/2010JC006644

Stone, G., 2000. Wave climate and bottom boundary layer dynamics with implications for offshore sand mining and barrier island replenishment in south-central Louisiana. U.S. Department of Interior, Minerals Management Service, Gulf of Mexico Region, New Orleans, LA, OCS Study, MMS 2000-053, 90 pp.

Stone, G., and J. Xu, 1996. Wave climate modeling and evaluation relative to sand mining on Ship Shoal, offshore Louisiana, for coastal and barrier island restoration. U.S. Department of Interior, Minerals Management Service, Gulf of Mexico Region, New Orleans, LA, OCS Study, MMS BOEM 96-059. 182 pp.

Stone, G.W., Condrey, R.E., Fleeger, J.W. and Khalil, S.M. 2009. Environmental investigation of the long-term use of Ship Shoal sand resources for large-scale beach and coastal restoration in Louisiana. U.S. Department of Interior, Minerals Management Service, Gulf of Mexico Region, New Orleans, LA, OCS Study, MMS 2009-024, 278 pp.

Styles, R., Glenn, S.M., 2000. Modeling stratified wave and current bottom boundary layers on the continental shelf. Journal of Geophysical Research 105(C10): 24119– 24139, doi:10.1029/2000JC900115.

Syvitski, J. P., Kettner, A. J., Overeem, I., Hutton, E. W., Hannon, M. T., Brakenridge, G. R., Day, J., Vörösmarty, C., Saito, Y., Giosan, L., & Nicholls, R. J., 2009. Sinking deltas due to human activities. Nature Geoscience, 2(10), 681.

Traykovski P, Trowbridge J, Kineke G, 2015. Mechanisms of surface wave energy dissipation over a high-concentration sediment suspension. Journal of Geophysical Research: Oceans 120(3):1638–1681. https://doi.org/10.1002/2014JC010245

Traykovski, P., P. L. Wiberg, and W. R. Geyer, 2007. Observations and modeling of wave-supported sediment gravity flows on the Po prodelta and comparison to prior

observations from the Eel shelf, Continental Shelf Research, 27, 375 – 399, doi:10.1016/j.csr.2005.07.008.
Traykovski, P., W. R. Geyer, J. D. Irish, and J. F. Lynch, 2000. The role of wave - induced density driven fluid mud flows for cross - shelf transport on the Eel River continental shelf, Continental Shelf Research, 20, 2113 – 2140, doi:10.1016/S0278-4343(00)00071-6.
Twilley, R.R., Bentley, S.J., Chen, Q.J., Edmond, D., Hagen, S., Lam, N., Willson, C., Xu, K.H., Braud, D.R., Peele, H., McCall, A., 2016. Co-evolution of wetland landscapes, flooding, and human settlement in the Mississippi River Delta Plain, Sustainability Science, 11, 711–731. DOI 10.1007/s11625-016-0374-4.
Vörösmarty, C. J., Syvitski, J., Day, J., De Sherbinin, A., Giosan, L., & Paola, C., 2009. Battling to save the world's river deltas. Bulletin of the Atomic Scientists, 65(2), 31-43.
Wang, J., Xu, K.H., Obelcz, J., Li, C., 2018, Forces Driving the Morphological Evolution of a Mud-Capped Dredge Pit, Northern Gulf of Mexico, Water, 10, 1001; doi:10.3390/w10081001.
Warner, J.C., Sherwood, C.R., Signell, R.P., Harris, C.K., Arango, H.G., 2008. Development of a three-dimensional, regional, coupled wave, current, and sediment-transport model Computers & Geosciences 34, 1284–1306.
Wiberg, P.L., Harris, C.K., 1994. Ripple geometry in wave-dominated environments, Journal of Geophysical Research, 99 (C1) (1994), 775-789.
Wiseman, Wm. J., Jr., Murray, S. P., Tubman, M. W., and Bane, J. M., 1975, Offshore physical oceanography: Technical Appendix III of Environmental Assessment of a Louisiana

Offshore Oil Port and Appurtenant Pipeline and Storage Facilities, v. 2. Final Rept., Louisiana Offshore Oil Port, New Orleans, Louisiana.

Williams, S.J., Arsenault, M.A., Buczkowski, B.J., Reid, J.A., Flocks, J.G., Kulp, M.A., Penland, S. and Jenkins, C.J., 2006. Surficial sediment character of the Louisiana offshore Continental Shelf region: a GIS Compilation. U.S. Geological Survey Open-File Report 2006-1195, online at http://pubs.usgs.gov/of/2006/1195/index.htm.

Xu, K., Wren, P.A., Ma, Y., 2020. Tidal and Storm Impacts on Hydrodynamics and Sediment Dynamics in an Energetic Ebb Tidal Delta. Journal of Marine Science and Engineering, 8, 810.

Xu, K.H., Bentley, S.J., Day, J.W., Freeman, A.M., 2019. A review of sediment diversion in the Mississippi River Deltaic Plain, Estuarine, Coastal and Shelf Science 225, 106241, https://doi.org/10.1016/j.ecss.2019.05.023.

Xu, K.H., Bentley, S.J., Robichaux, P., Sha, X., Yang, H., 2016b. Implications of Texture and Erodibility for Sediment Retention in Receiving Basins of Coastal Louisiana Diversions, Water, 8, 26; doi:10.3390/w8010026.

Xu, K.H., Harris, C.K., Hetland, R.D., Kaihatu, J. M., 2011. Dispersal of Mississippi and Atchafalaya Sediment on the Texas-Louisiana Shelf: Model Estimates for the Year 1993, Continental Shelf Research, 31, 1558-1575. doi:10.1016/j.csr.2011.05.008.

Xu, K.H., Mickey, R.C., Chen, Q.J., Harris, C.K., Hetland, D., Hu, K., Wang, J., 2016a. Shelf Sediment Transport during Hurricanes Katrina and Rita, Computers& Geosciences, 90, 24–39. http://dx.doi.org/10.1016/j.cageo.2015.10.009.

Xu, K.H., Sanger, D., Riekerk, G., Crowe, S., Van Dolah, R., Wren, P., Ma, Y., 2014. Seabed texture and composition changes offshore of Port Royal Sound, South Carolina before and after the dredging for beach nourishment, Estuarine, Coastal and Shelf Science, 149, 57-67. DOI: 10.1016/j.ecss.2014.07.012.

Xue, Z., Wilson, C., Xu, K., Bentley, S., Liu, H., 2021. Sandy Borrow Area Sedimentation—Characteristics and Processes Within South Pelto Dredge Pit on Ship Shoal, Louisiana Shelf, USA. Estuaries and Coasts, https://doi.org/10.1007/s12237-021-00975-6

Zhang, X.D., Lu, Z.Y., Jiang, S.H., Chi, W.Q., Zhu, L.H., Wang, H.M., Lv, K., Wang, B.Y., Yang, Z.S., 2018a. The progradation and retrogradation of two newborn Huanghe (Yellow River) Delta lobes and its influencing factors. Marine Geology, 400, 38-48.

Zhang, X. D., Zhang, Y. X., Zhu, L. H., Chi, W. Q., Yang, Z. S., Wang, B. Y., Lv, K., Wang, H. M., Lu, Z. Y., 2018b. Spatial-temporal evolution of the eastern Nanhui mudflat in the Changjiang (Yangtze River) Estuary under intensified human activities. Geomorphology, 309, 38-50.

Zhang, X. D., Fan, D. D., Yang, Z. S., Xu, S. M., Chi, W. Q., Wang, H. M., 2020. Sustained growth of river-mouth bars in the vulnerable Changjiang Delta. Journal of Hydrology, 590, 125450.

Zang, Z., Xue, Z. G., Xu, K.H., Ozdemir, C. E., Chen, Q., & Bentley, S. J., et al., 2020. A numerical investigation of wave‐supported gravity flow during cold fronts over the Atchafalaya shelf. Journal of Geophysical Research: Oceans, 125, e2019JC015269. https://doi.org/10.1029/2019JC015269

Table 1

Station	Sensor	Provider	Orientation	Measuring parameters	Measuring elevations (mab)	Sampling interval (min)	Sampling duration (min)
R1	OBS3A	Campbell Scientific, USA	side looking	T, S, P and Turbidity	0.52	15	1
R1	OBS5	Campbell Scientific, USA	side looking	Turbidity	0.10	15	1
R1	ADV Ocean 5MHz	Sontek, xylem	downward looking	T, V and P	0.63	60	20
R1	Wave Gauge, 10Hz	Ocean Sensor Systems, USA	downward looking	T and P	0.35	60	20
R1	ADCP, Sentinel 1200 kHz	Teledyne RD Instruments	upward looking	T, V and Wave	0.97 - 8.00, with 0.5 m bin size	60	20
CSI06	ADCP, Sentinel 600 kHz	Teledyne RD Instruments	upward looking	T, V and Wave	5.13 – 19.00, with 1 m bin size	60	20

Table 2

Period	Date	Wind speed of CSI06 (m/s)	Wind direction of CSI06 (°)	Max alongshore current near sea surface at R1 (m/s)	Wave height at R1 (m)	Wave period at R1 (s)	Tide at R1	Cum. longshore flux at R1 (kg/m/s)
P1	May 27-29, 2016	6.9	150.5 (SE)	-0.43 (west)	0.85	4.1	Spring	-83.3 (west)
P2	June 7-9, 2016	4.0	variable and rotating	-0.25 (west)	0.58	6.5	Spring	-52.5 (west)
P3	July 4-6, 2016	6.6	207.7 (SW)	0.32 (east)	0.73	3.8	Spring	20.6 (east)

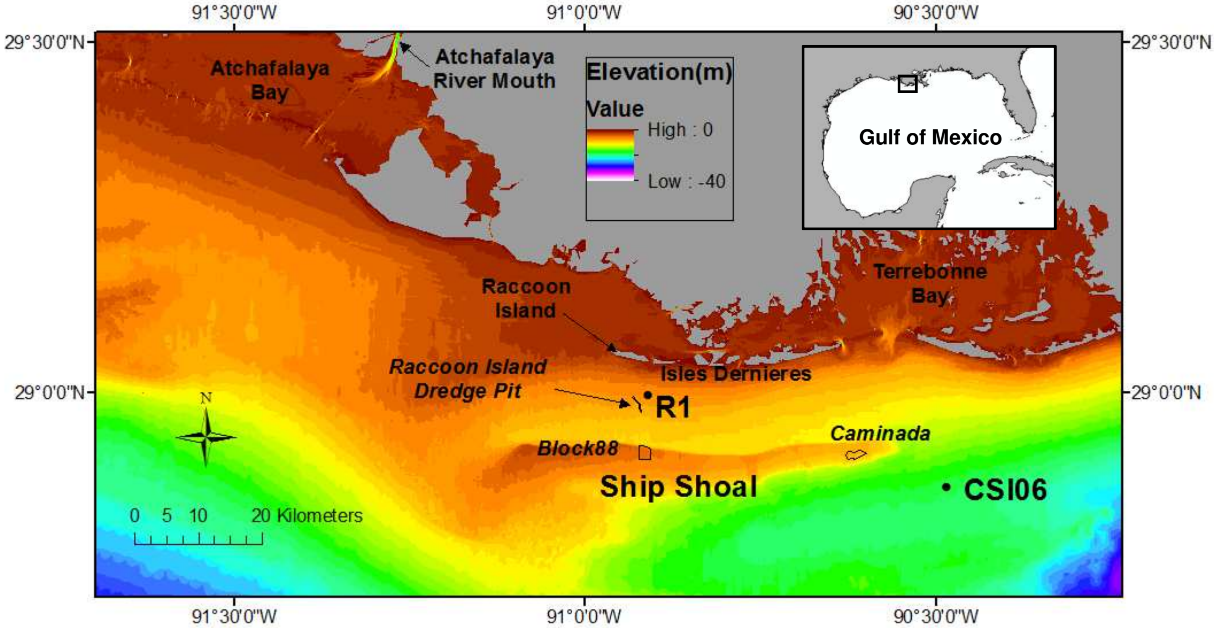
91°30'0"W
91°0'0"W
90°30'0"W
29°30'0"N
29°0'0"N
Atchafalaya Bay
Atchafalaya River Mouth
Elevation(m)
Value
High : 0
Low : -40
Gulf of Mexico
Raccoon Island
Terrebonne Bay
Raccoon Island Dredge Pit
Isles Dernieres
R1
Caminada
Block88
Ship Shoal
CSI06
N
0 5 10 20 Kilometers

Fig. 1

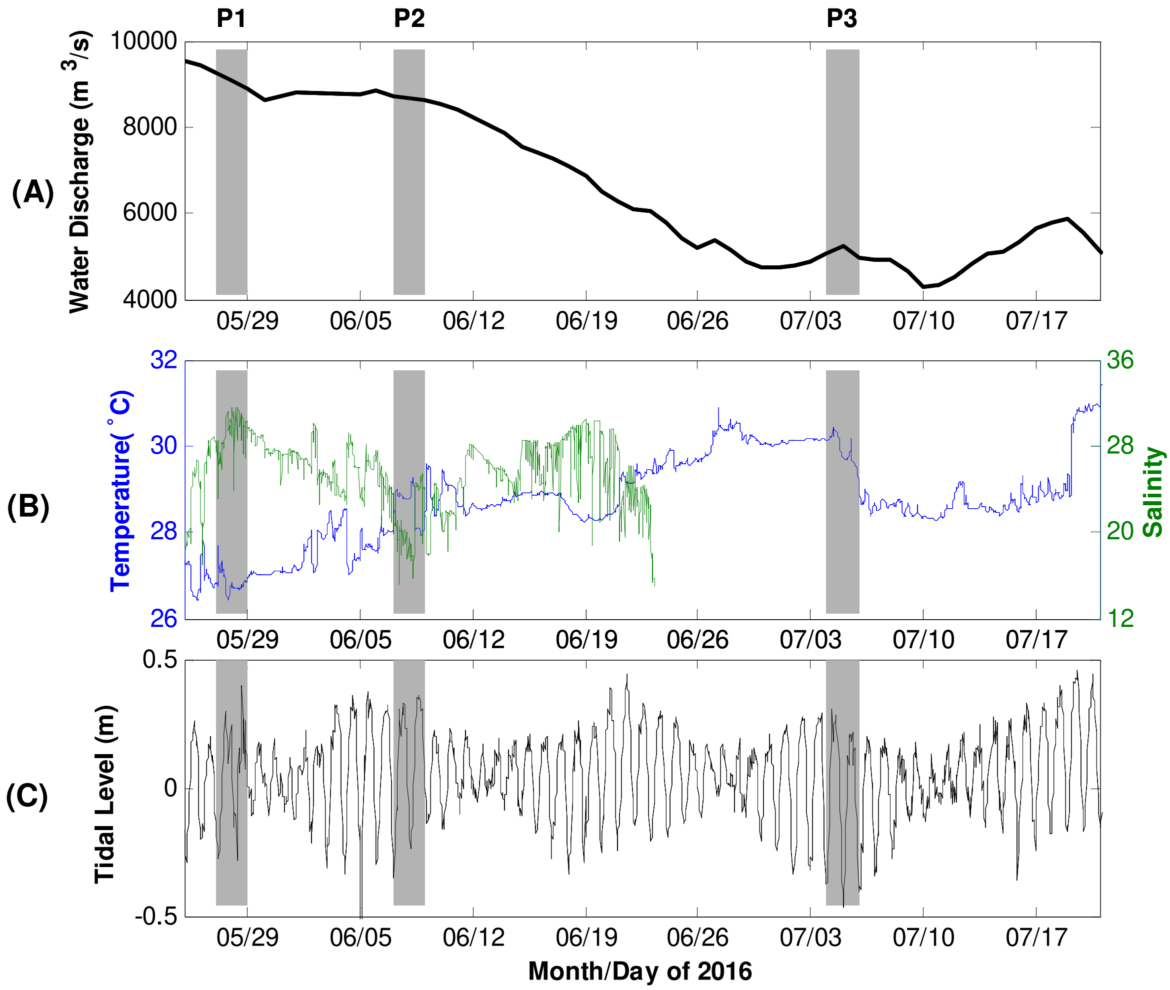
P1
P2
P3
(A)
Water Discharge (m 3/s)
10000
8000
6000
4000
(B)
Temperature(°C)
32
30
28
26
Salinity
36
28
20
12
(C)
Tidal Level (m)
0.5
0
-0.5
05/29
06/05
06/12
06/19
06/26
07/03
07/10
07/17
Month/Day of 2016

Fig. 2

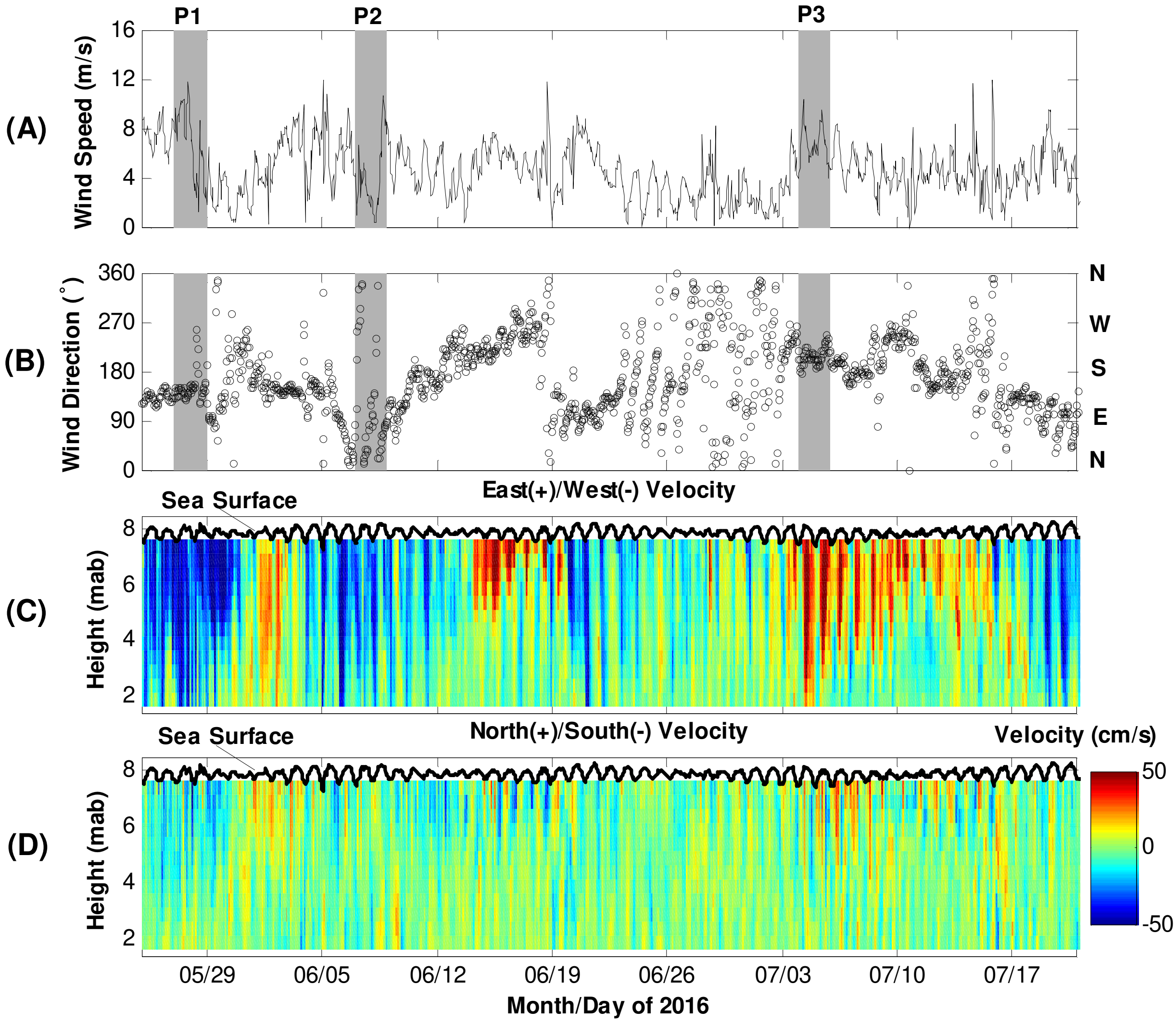
P1
P2
P3
(A)
Wind Speed (m/s)
(B)
Wind Direction (˚)
N
W
S
E
N
East(+)/West(-) Velocity
Sea Surface
(C)
Height (mab)
North(+)/South(-) Velocity
Sea Surface
Velocity (cm/s)
(D)
Height (mab)
05/29
06/05
06/12
06/19
06/26
07/03
07/10
07/17
Month/Day of 2016

Fig. 3.

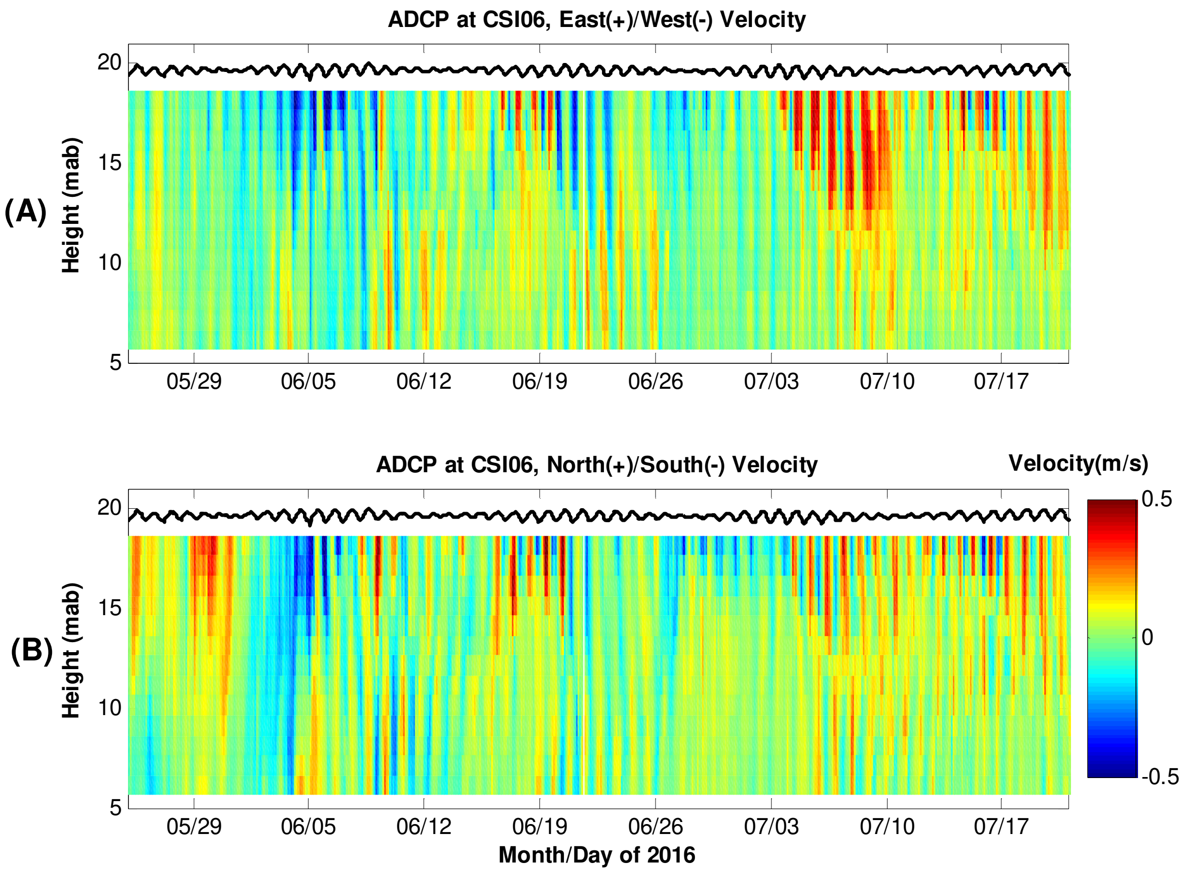

ADCP at CSI06, East(+)/West(-) Velocity
(A)
Height (mab)
20
15
10
5
05/29
06/05
06/12
06/19
06/26
07/03
07/10
07/17
ADCP at CSI06, North(+)/South(-) Velocity
Velocity(m/s)
0.5
0
-0.5
(B)
Height (mab)
Month/Day of 2016

Fig. 4.

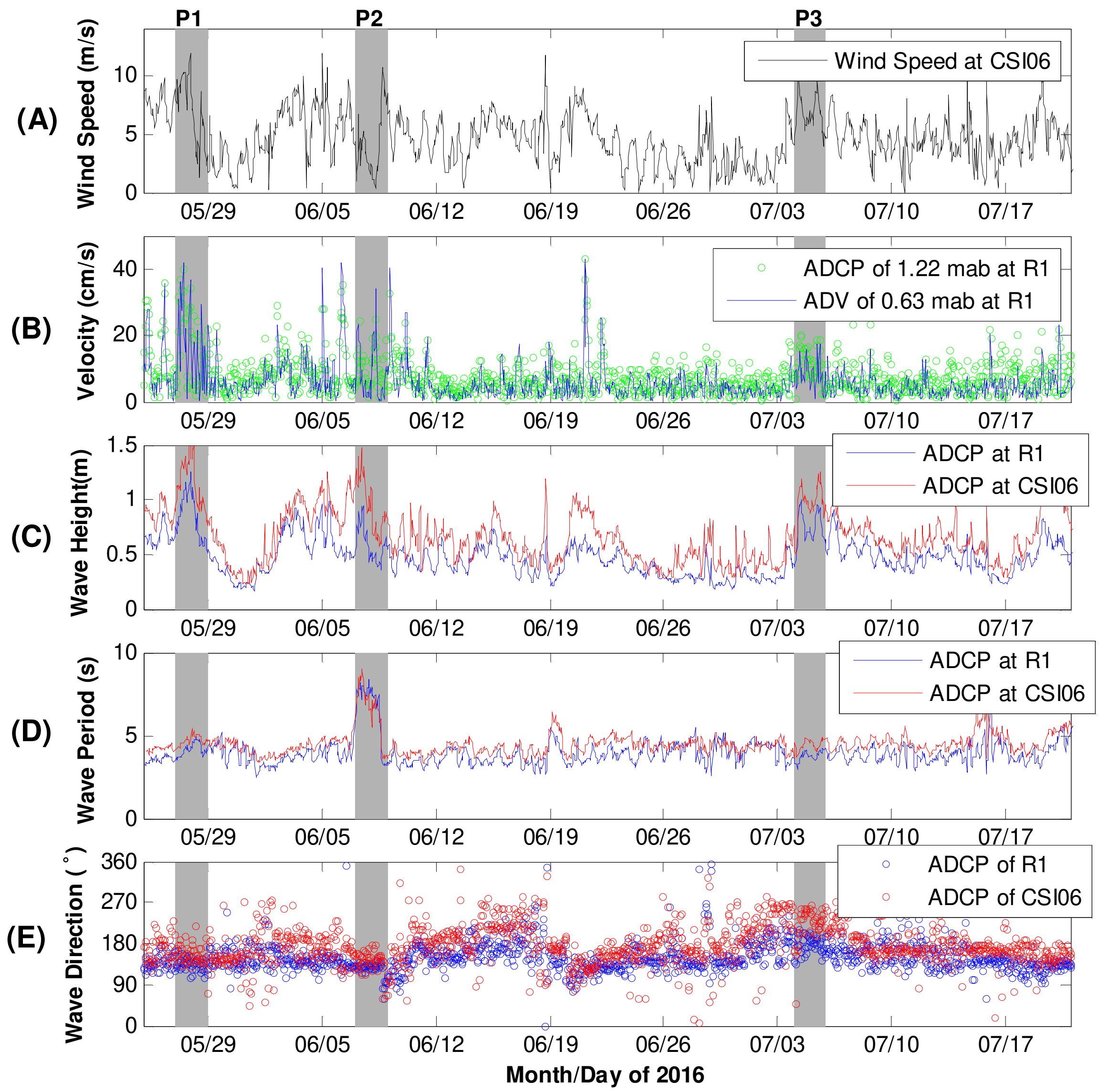

P1
P2
P3
(A)
Wind Speed (m/s)
Wind Speed at CSI06
(B)
Velocity (cm/s)
ADCP of 1.22 mab at R1
ADV of 0.63 mab at R1
(C)
Wave Height(m)
ADCP at R1
ADCP at CSI06
(D)
Wave Period (s)
ADCP at R1
ADCP at CSI06
(E)
Wave Direction (°)
ADCP of R1
ADCP of CSI06
05/29
06/05
06/12
06/19
06/26
07/03
07/10
07/17
Month/Day of 2016

Fig. 5.

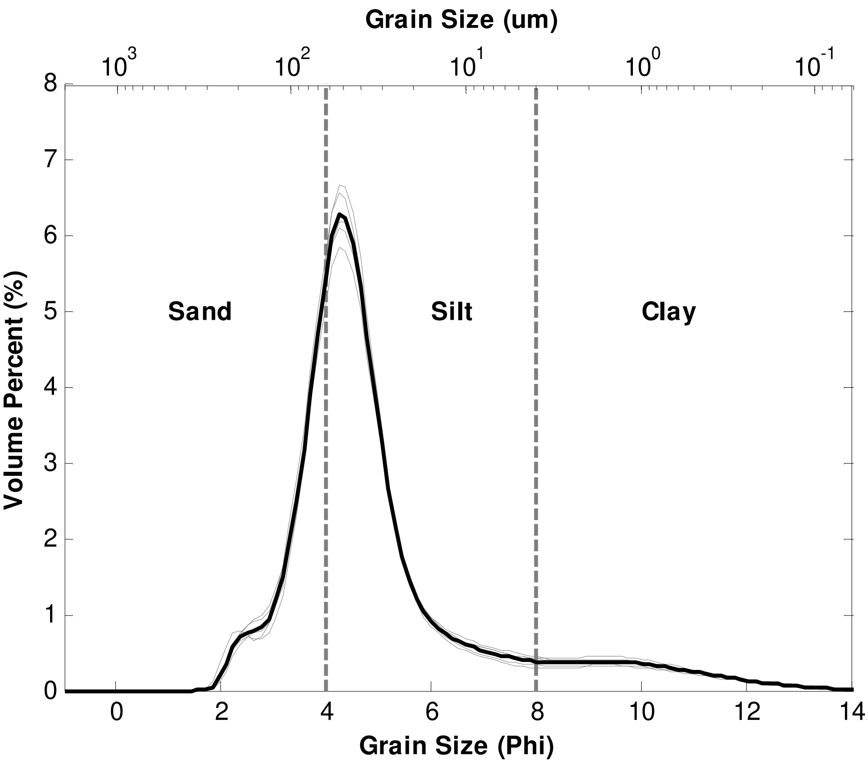

Grain Size (um)
10^3
10^2
10^1
10^0
10^-1
Volume Percent (%)
0
1
2
3
4
5
6
7
8
Sand
Silt
Clay
0
2
4
6
8
10
12
14
Grain Size (Phi)

Fig. 6.

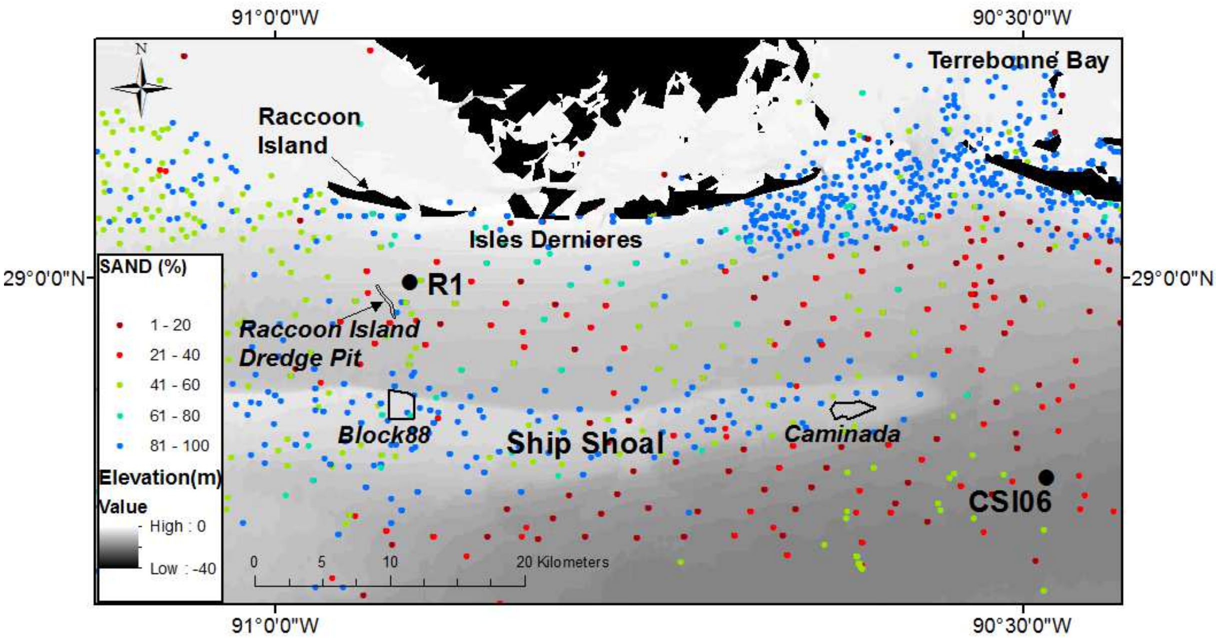
91°0'0"W
90°30'0"W
29°0'0"N
N
Raccoon Island
Terrebonne Bay
Isles Dernieres
R1
Raccoon Island Dredge Pit
Block88
Ship Shoal
Caminada
CSI06
SAND (%)
1 - 20
21 - 40
41 - 60
61 - 80
81 - 100
Elevation(m)
Value
High : 0
Low : -40
0
5
10
20 Kilometers

Fig. 7.

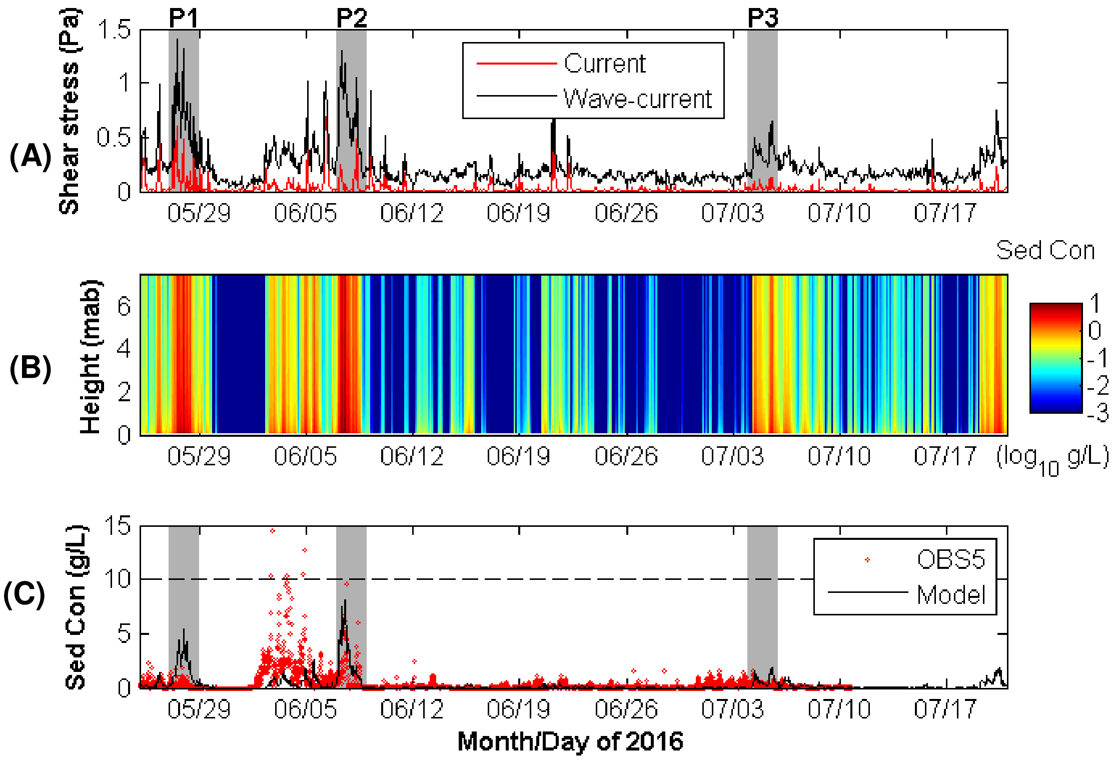
P1
P2
P3
Current
Wave-current
(A)
Shear stress (Pa)
1.5
1
0.5
0
05/29
06/05
06/12
06/19
06/26
07/03
07/10
07/17
Sed Con
(B)
Height (mab)
6
4
2
0
1
0
-1
-2
-3
(log10 g/L)
(C)
Sed Con (g/L)
15
10
5
0
OBS5
Model
Month/Day of 2016

Fig. 8.

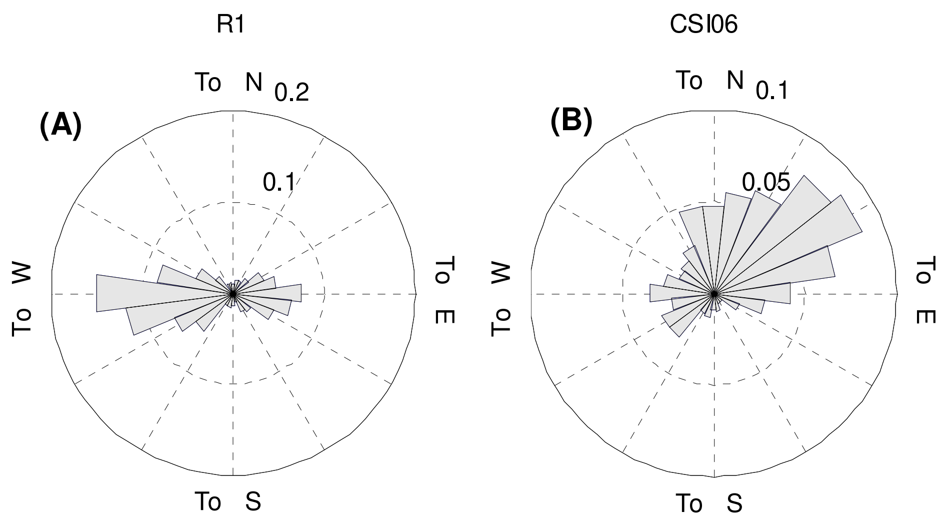

Fig. 9.

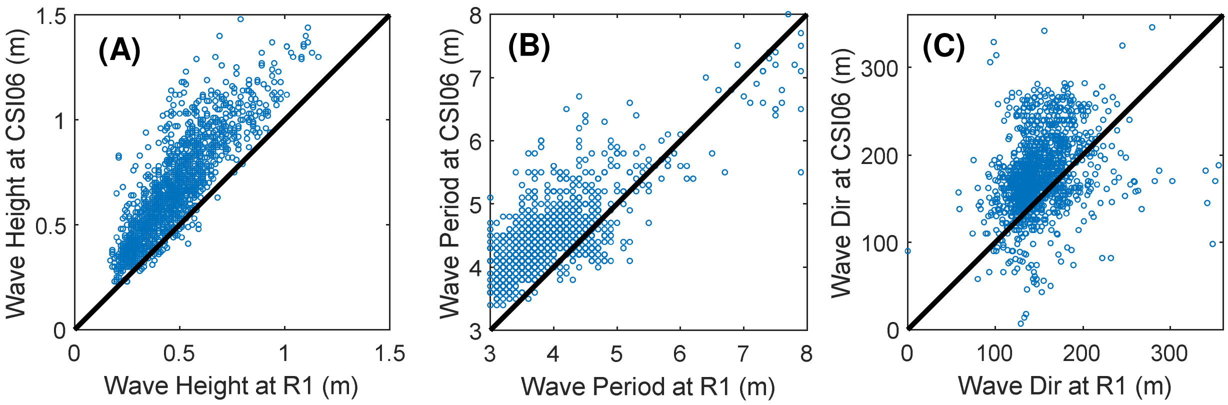
(A)
Wave Height at CSI06 (m)
Wave Height at R1 (m)
0
0.5
1
1.5
(B)
Wave Period at CSI06 (m)
Wave Period at R1 (m)
3
4
5
6
7
8
(C)
Wave Dir at CSI06 (m)
Wave Dir at R1 (m)
0
100
200
300

Fig. 10.

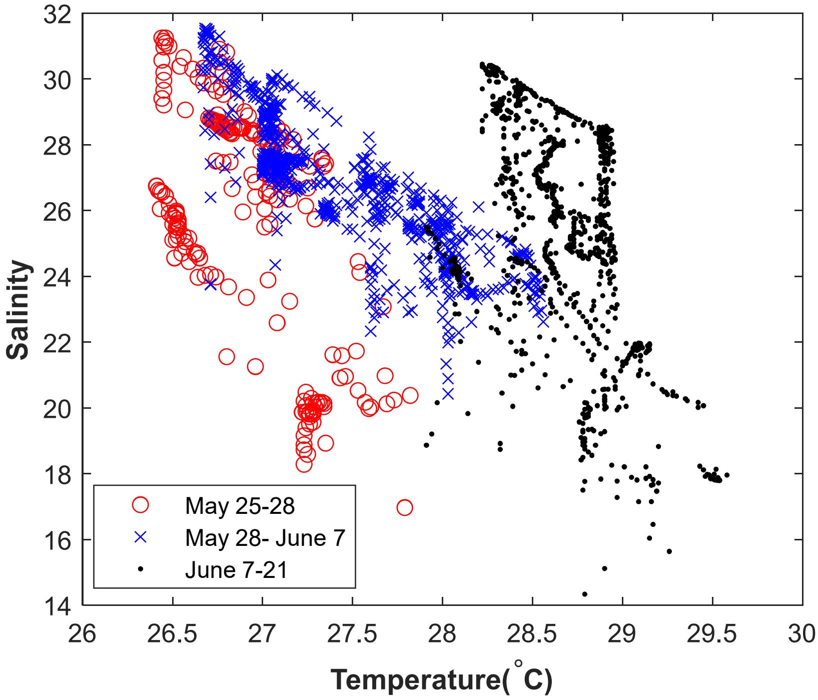

Salinity
Temperature(°C)
32
30
28
26
24
22
20
18
16
14
26
26.5
27
27.5
28
28.5
29
29.5
30
May 25-28
May 28- June 7
June 7-21

Fig. 11.

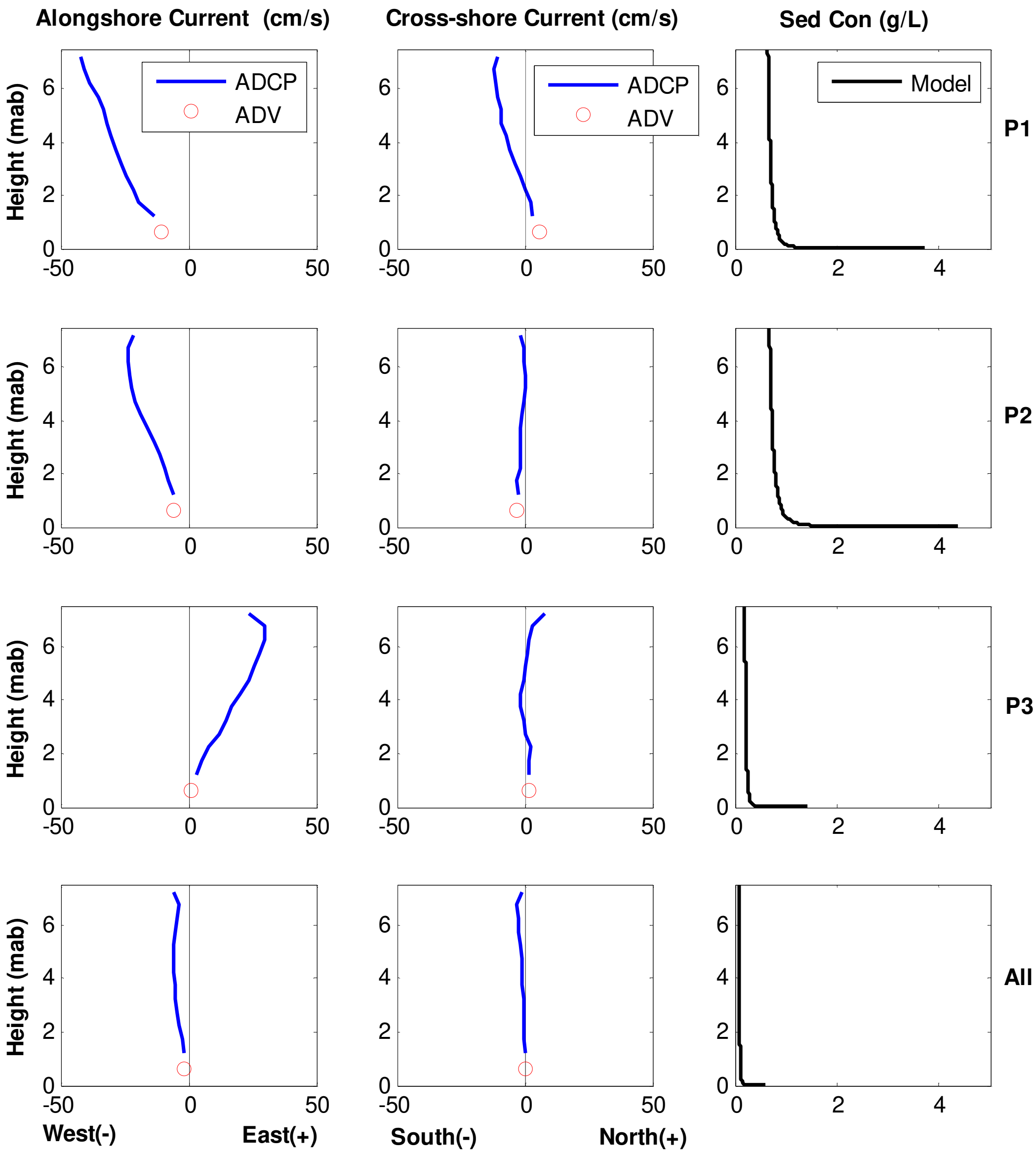
Alongshore Current (cm/s)
Cross-shore Current (cm/s)
Sed Con (g/L)
Height (mab)
ADCP
ADV
Model
P1
P2
P3
All
0
2
4
6
-50
50
West(-)
East(+)
South(-)
North(+)

Fig. 12.

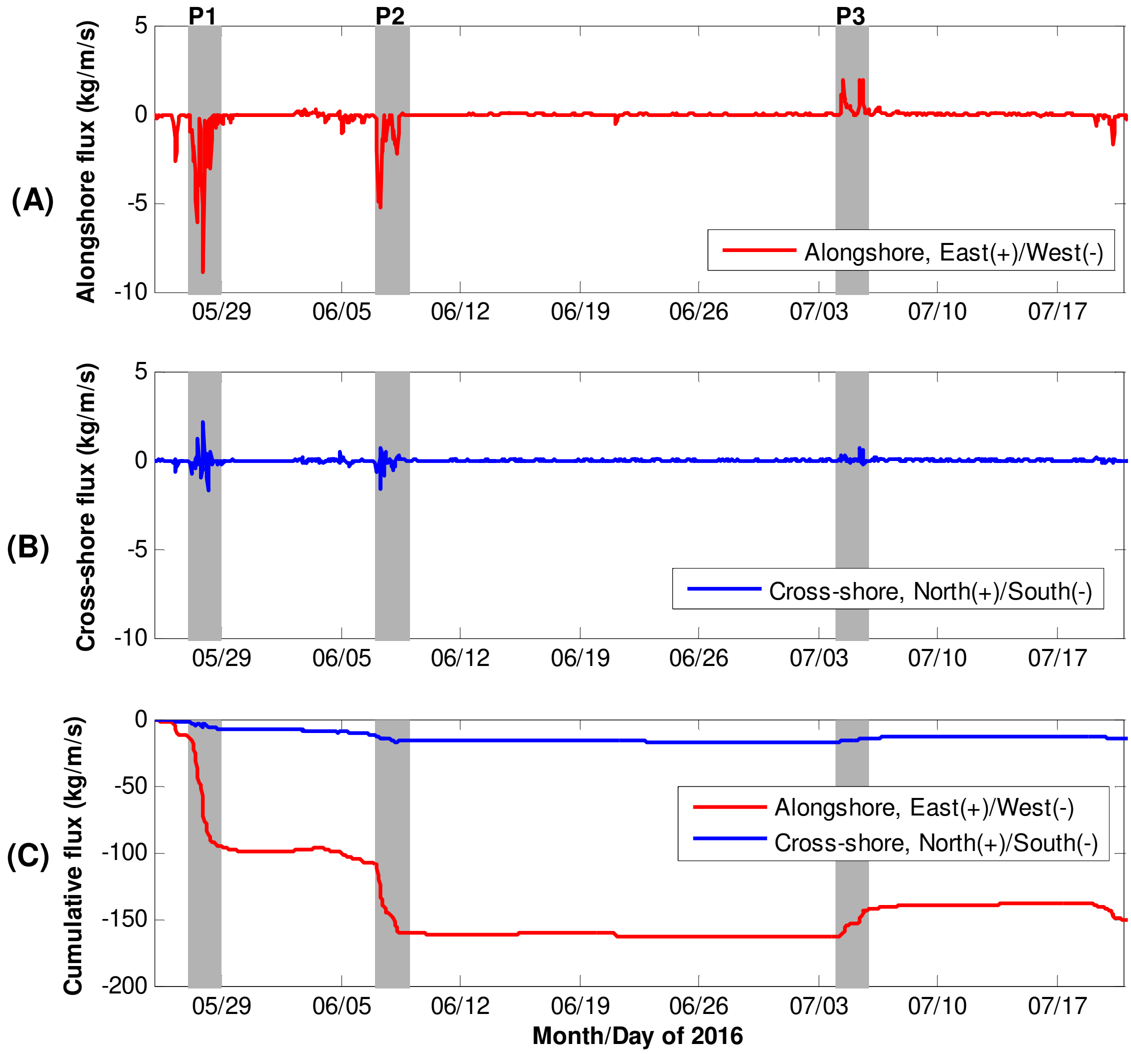
P1
P2
P3
(A)
Alongshore flux (kg/m/s)
Alongshore, East(+)/West(-)
(B)
Cross-shore flux (kg/m/s)
Cross-shore, North(+)/South(-)
(C)
Cumulative flux (kg/m/s)
Alongshore, East(+)/West(-)
Cross-shore, North(+)/South(-)
05/29
06/05
06/12
06/19
06/26
07/03
07/10
07/17
Month/Day of 2016

Fig. 13.